Gold-Indium Intermetallic Compounds: Properties and Growth Rates

Jane E. Jellison
Code 313:
Materials Control and Applications Branch (MC&AB)

8 November 1979

Note: Jane Jellison originally composed this as a memo to the TIROS Project to describe her study of failures on gold-ball bonds in detectors made by Honeywell for a TIROS satellite. Henning Leidecker recast her memo into the present article in July 2003.

1 Summary

The growth rate and characteristics of gold-indium intermetallic compounds were investigated in order to determine the impact of their presence in the lead wire bonds to HgCdTe detector chips. It was concluded that:

1. The major compound formed is $AuIn_2$, which is very friable but a good electrical conductor.
2. Significant amounts of compound are very likely to form during detector fabrication.
3. The growth rate of this compound is not negligible at room temperature.
4. There is no known non-destructive method to determine whether a properly functioning device has very weak bonds.
5. An equation predicting growth at low temperatures is presented.

2 Introduction

As a result of gold-indium intermetallic compound formation observed in lead wire bonds to HgCdTe detector chips in Honeywell IR detectors, a test program was outlined to determine the conditions under which such growth would occur to a significant degree and what the mechanical and electrical properties of the compounds would be.[1] The objectives of the program were outlined and preliminary results were reported in a memo, dated May 15, 1979, from the MC&AB addressed to the TIROS Project Office. These objectives were stated as:

1. Determine growth rate and characteristics of Au-In intermetallics at various temperatures.
2. Determine the physical and mechanical properties of Au-In intermetallics and their effect on bond strengths.

The test plan to achieve these objectives consisted of the following segments:

1. Preparation and Testing of Au-In Bonds
   - Prepare gold wire bonds on indium coated substrate, hold at temperature, pull test, and examine for intermetallic compound growth.
2. Preparation and Testing of AuIn and $AuIn_2$ Intermetallic Compounds
   - Prepare bulk samples of these compounds.
   - Determine mechanical properties, fracture mode, and electrical resistance.
3. Growth Rate Studies of Au-In Intermetallic Compounds
   - Prepare Au-In couple for optical microscope hot stage for real-time viewing of intermetallic growth.
   - Prepare Au-In couples suitable for both metallographic cross-sectioning and SEM observation. Hold each couple at a fixed temperature, with different couples held at different temperatures and observe periodically.
4. Growth Rate Curve Determination
   - From data obtained, extrapolate growth characteristics to room temperature and below so as to evaluate what detector bonds might contain.

[1] Note added by HL: A mixture of gold and indium is denoted Au-In. Specific compounds form in this mixture, including AuIn and $AuIn_2$. This distinction between Au-In and AuIn has been made throughout this article.

The present report details these investigations, and presents a summary of the conclusions and recommendations obtained therefrom.

3 Preparation and Testing of Au-In Bonds

Two groups of bonds were prepared, to be observed at temperature in a vacuum furnace hot-stage metallograph. Two beryllium-copper specimens of the appropriate dimensions for the hot stage were first coated with a RF-sputtered layer of nichrome to act as a barrier between the indium and the Be-Cu substrate. Next, indium was melted onto this surface and spread with a spatula (no indium target was available for the RF coater). This method left a rather thick indium coating, and considerable difficulty was encountered in thermo-sonically bonding 1 mil gold wires to it. Most of them were deeply buried in the indium.

One bond was pull tested prior to elevated temperature exposure. Failure was in the wire at a load of 6 g_f. After inserting specimen #1 in the vacuum furnace, the temperature was raised to 140°C. The temperature was lowered to 120°C at night to avoid accidental overheating and melting of the indium due to the normal increase in line voltage which occurs at the end of the workday. The specimen was removed for SEM examination and bond pull testing after a total of 73 hours at 140°C plus 97 hours at 120°C.

The first reaction product was noticed almost immediately after the test was started. Within one hour, the gold wires near the indium contact areas were covered with a surface film which extended up the wire away from the gold-indium interface. This material continued to grow in extent and in thickness throughout the test.

After the initial reaction, further visual examination became more difficult because of the 3-dimensional nature of the areas of interest and the lack of depth of field in the optical viewing system. However, SEM photographs of each bond were obtained before and after temperature exposure and bond testing and are presented in Figures 2 through 7. An overall view of the specimen surface, Figure 1, shows the layout of the bond pairs lA-B and 1C-D. Bond lA, Figure 2, shows that after the exposure to temperature the surface of the gold ball, as well as the area immediately adjacent to the indium, was covered with intermetallic compound. The higher magnification photo shows that crystalline growth has filled the gap between the ball and the indium. The other half of this pair, Bond 1B, Figure 3, shows the upward movement of the compound growth as well as the pushing aside of the indium caused by the increasing volume of compound. When this bond pair was pull tested, Bond 1B lifted at a force of 2.3 g_f.

Most of the failed interface area on the wire was covered with granular material similar to that which formed on the exposed surfaces, Figure 4, indicating that

the indium beneath this area had been totally consumed by the reaction at the heel of the bond where the compound-coated wire had still been in contact with bulk indium. An area of ductile failure in the indium is shown in the bottom of Figure 4.

Similar photographs of bond pair 1C-D are presented in Figures 5 through 7. Bond lC shows a coating of intermetallic compound which approximately doubles the apparent diameter of the wire and which extends several micrometers up the wire, illustrating the mobility of the indium under these conditions. Upon pull testing, Bond 1D lifted at a force of 2.0 g_f. The whole surface of the gold ball showed extensive compound formation, with small areas of ductile indium fracture surface interspersed with granular intermetallic compound.

In summary, intermetallic growth is rapid at these elevated temperatures, and the indium is very mobile. Extensive compound formation occurred some distance away from the original gold-indium interface, and bond strength was reduced from 6 to 2 grams-force.

4 Preparation and Testing of AuIn and $AuIn_2$ Intermetallic Compounds

4.1 Procedure for Preparing Specimens

Place required amounts of Au and In wire in Pyrex tubes, 4 mm O.D. × 50 mm long. Evacuate tubes, backfill with nitrogen, re-evacuate to one microtorr and seal off. Place tubes in furnace, heat to 550±2°C (above melting point of AuIn and $AuIn_2$), hold 1.5 hours, furnace cool. Anneal at 475±2°C for 20 hours (below melting point of compounds).

4.2 Metallographic Examination

The resulting ingots from the above preparation procedure measured about 3 mm in diameter and were about 10 mm long. One end was cut off and prepared for metallographic examination and microhardness measurements.

The compositions had purposely been calculated to fall slightly within the eutectic region of the phase diagram whose end points are AuIn and $AuIn_2$ (see Figure 8) so as to avoid complication due to the presence of other phases. Figures 9 and 10 show the microstructures of the two alloys in the unetched and etched conditions. The nominally AuIn specimen shows a matrix of this compound with some $AuIn_2$ present. The reverse is true for the $AuIn_2$ specimen. (The $AuIn_2$ phase etches brown with the etchant selected.)

Compound	Present Study	Reference (1)
AuIn	250	273
$AuIn_2$	52	77
Au_9In_4	—	368

Table 1: Microhardness measurments made on present specimens and reported in the literature. (Values are in "Diamond Pyramid Hardness" units.)

Some cracks were noted in the Au-In specimen, propagating through both phases (see Figure 11). It is not known if these cracks formed during the alloy preparation process or during the sectioning prior to metallographic mounting. In either event, the crack presents a brittle appearance.

Microhardness measurements were made on both phases and are compared with published values in Table 1.

4.3 Mechanical Properties

Since it was suspected that both compounds were brittle, no attempt was made to form the ingots into a more convenient shape for mechanical testing. One end had been squared off by the cutting off of the metallographic sample, and it was decided to run a shear test to remove the other rounded end, leaving a cylindrical section for further testing. Accordingly, a fixture was designed and built consisting of a fixed block with a suitable hole through it, and a pusher with a corresponding hole to accommodate the other end of the specimen. The fixture was placed in an Instron Universal Testing machine, and the load required to shear the end off was recorded: see Table 2 and the sketch.

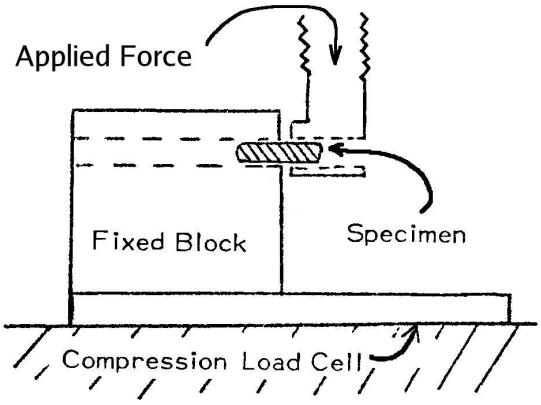

Compound	Maximum Load	Shear Stress
AuIn	139 lb.	10,300 psi
$AuIn_2$	50 lb.	3,700 psi

Table 2: Resistance to shearing measured for present specimens.

In addition to the main fracture surface, the $AuIn_2$ specimen exhibited several additional cracks parallel to the fracture face.

SEM fractographs of both specimens are shown in Figure 12. In both specimens the overall fracture appearance was very brittle with little or no plastic deformation. Fracture was largely by transgranular cleavage with numerous subcracks in evidence. Some areas of the Au-In specimen failed through the $AuIn_2$ colonies in the grain boundaries.

4.4 Electrical Resistance

The remainder of the ingots were used to measure their electrical resistance. For both AuIn and $AuIn_2$ the resistance was measured as less than 0.01 ohms, which was the lower limit of the meter used. [HL: This places an upper limit of about 1 mΩ on the resistivity; later work by others established the resistivity at 300 K as about 8.8 $\mu\Omega$·cm, very nearly 4.0 times that of gold.]

5 Growth Rate Studies of Au-In Intermetallic Compounds

5.1 Specimen Preparation

Gold wires were threaded through the sides of silicone rubber molds so that when the molds were filled with molten indium the wires would run through the centers of the resulting ingots. Some of the molds were pre-heated to insure that the indium would flow under and around the gold wires so as to surround them completely. Others were not preheated, so that the indium froze upon contacting the wires and did not completely cover them (see sketch).

The Type A ingots (gold wire completely surrounded by indium) were sliced with a razor blade into approximately 3 mm thick sections. Several of these were put into an oven at each test temperature and were withdrawn one at a time at various time intervals for metallographic examination of intermetallic layer thickness.

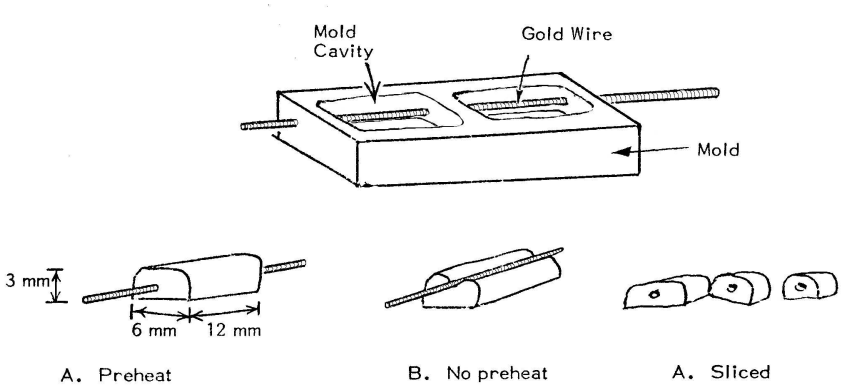

One of the second type of specimens, with a portion of the wire exposed, was also held at each temperature, and was periodically removed for SEM examination of the Au-In interface. These specimens were put back in the oven after each SEM examination.

In addition, one ingot slice was mounted for direct observation in an optical microscope vacuum hot stage. This specimen was held at 140°C for thirty-five hours and was then examined in the SEM and metallographically cross-sectioned. This procedure was carried out first and at a high temperature to get an indication of what features could be seen and as a trial run for the SEM and sectioning procedures.

5.2 Description of Results: Hot Stage Specimens

By the time the hot stage specimen had reached temperature and the camera had been readied, (about 15 minutes), a noticeable growth had occurred at the interface between the gold wire and the surrounding indium, Figure 13. (The razor cut surface was quite rough, but one segment of the interface was acceptable for microscopic observation.) As time progressed, the growth extended both outward over both the gold and indium surfaces and upward, forming a rounded ridge. The growth was dark gray in color, and appeared somewhat grainy. After about 14 hours, a fissure appeared revealing larger, blocky grains below the surface film: see the center middle image of Figure 13. This layer continued to grow in width for the remainder of the test. At this time the surface had become too irregular for useful microscopic examination: see the center bottom image, and the right top and middle image, of Figure 13. A SEM photo corresponding to the last optical photo is shown: see the right bottom image in

Figure 13.

Figure 14 compares higher magnification SEM photos with a photomicrograph of the specimen after it had been ground, polished, and etched. In the polished condition, the layer of fine grainy material on the gold wire surface has been removed. Once the surface layer has been removed, the blocky grain structure is seen to extend from the gold wire to the indium matrix. The grains do not appear to be bonded together very strongly.

5.3 Description of Results: SEM and Metallographic Specimens

Specimens were held at temperatures of 40, 60, 80, 100, 125, and 140°C. At the higher temperatures the reactions proceed rapidly; while at 40°C observation intervals of weeks or months are required to note significant changes.

A specimen held at 125°C for 97 hours is shown in Figure 15. The upper two photographs show one end of the gold wire where it has been pulled away from the indium block. A heavy layer of Au-In intermetallic compound has formed where the wire had been in contact with the indium. A second area where the wire had not been pulled out is shown in images `c` to `e` of Figure 15.

The compound layer extends on the gold surface beyond the edge of the indium and the appearance of the "top" surface of this layer is quite different from that of the "side wall". Apparently, the force of the growing compound layer has pushed the wire up out of the indium block, exposing the surface characterized by blocky grains which had previously been in contact with the bulk indium. The leading face, or "wall" of the compound layer is finer grained and/or columnar in appearance.

This dual surface morphology is also seen in a sample held 144 hours at 125°C, Figure 16. In addition, a crack has formed within the blocky structure along either side of the wire. A cross-section through a different specimen held for 500 hours at 125°C, Figure 17, shows many intergranular cracks, voids, and fissures within the compound layer. Layer growth has proceeded unevenly, resulting in a non-circular cross section of the unconsumed gold wire. This is probably the result of air bubbles or voids in the indium near the gold wire from the casting process. In the etched condition, the compound layer is seen to be formed of crystals of $AuIn_2$ of various sizes, smaller and columnar near the gold wire and large and blocky farther out. Verification of the compound composition was obtained by energy dispersive X-ray analysis (EDX). Some of the breakup near the outside of the layer is very likely due to damage during the sectioning process (early specimens were sliced after exposure to temperature; later ones were pre-cut) but some of the voids and cracks would correspond to those seen on the surface of the specimen pictured in Figure 16.

As the test temperature was lowered, the growth rate decreased, and it became increasingly easier to monitor compound growth in a given area as a function of time at temperature. Figure 18 illustrates the 100°C specimen at various time intervals and magnifications. At the start of the test, see images `a` and `b` in Figure 18, no compound was visible. The area shown in image `b` of Figure 18 was selected for a "before" photograph because the gold and indium were in close contact at the center of the field of view. After 72 hours, a colony of compound had obligingly formed at that spot, as shown in images `c` and `d` of Figure 18. As time passed, growth underneath the wire started to force the wire up out of the indium block, carrying this colony with it, see images `e` and `f` of Figure 18 (240 hours). After 312 hours, contact had been lost between the colony and the indium and growth in this area ceased except for a small area at the top of the photo where a ribbon-like feature connects the two. At 568 hours, images `h` and `i` of Figure 18, continued growth elsewhere has increased the separation and the ribbon has extended in length. The composition of the ribbon was not determined because its location made it inaccessible to the X-ray analyzer.

Metallographic examination of cross sections of fully embedded wires exposed to 100°C are shown in Figure 19. Layer thickness was more uniform than at higher temperatures and contained fewer voids. Virtually all of the layer appeared to be fine grained $AuIn_2$ with some intergranular cracks.

The 80°C SEM specimen provided a graphic illustration of the force exerted by continued intermetallic compound growth. Image `a` in Figure 20, taken after 164 hours at 80°C, shows a feature which can be visualized as an indium angel fish nibbling some intermetallic algae. As the compound continued to grow, the front part of the fish's face became wrinkled and compressed. By 357 hours, the mouth was pushed back close to the eye and a crease in the indium has formed just in front of the eye. As the process continued, the face was totally consumed and new creases were formed in the bulk indium. It was observed that the new growth appears on the gold side of the intermetallic compound layer, with previously formed features being displaced toward the indium side. In Figure 21, also taken from the 80°C SEM sample, this is particularly evident because of the development of columnar or elongated features at 357 hours which are recognizable in the 1072 hour photograph more than half-way up the compound layer face (circled areas). Also noted was the displacement of the indium ball at the apex of the compound stack: it has been forced into the bulk of the indium by 1072 hours.

Some of the regions of elongated features noticed at 900 and 1072 hours appeared to be extremely ductile, Figure 22. It is believed that this is a surface layer, possibly oxidized, and is not representative of the bulk compound layer. Image `b` in Figure 22 shows some of the blocky structure visible through a hole in the veil of ductile material (arrow at left center) and similar indications were noted elsewhere on this specimen.

To determine the correlation between surface features and subsurface layer

growth, the 80°C SEM specimen was cross-sectioned after 1072 hours at temperature. Figure 23 compares a SEM photograph with an optical photomicrograph of a section through the general area of the SEM photo. The fissure in the compound on the right hand side of the wire in the SEM photo appears as a crack in the cross section. This crack extends a short distance into the bulk compound layer and is believed to be caused by stresses imposed by the extensive subsurface compound growth. A SEM photo and a cross section through a region showing the elongated ductile features is presented in Figure 24. Again the fissure can be seen in both views, but the veil material is apparently too superficial as well as too delicate to be seen in cross section. Etching revealed the blocky grain structure common to all specimens at all temperatures. More intergranular cracking occurred near the surface than in the bulk of the layer, again apparently because of higher unbalanced stresses in this area.

Figures 25 and 26 compare surface morphology at 80°C and at 40°C in areas where a relatively thin layer of indium had spread out over the gold surface. Growth characteristics appear to be the same for both temperatures. On the 80°C specimen after 357 hours, image c of Figure 25, the indium layer has been essentially used up, and the blocky intermetallic structure can be seen through the remaining thin layer of indium and/or indium oxide (arrow).

This latter phenomenon is illustrated in Figures 27 and 28, which are both of areas where small patches of indium about 10 micrometers across were isolated on the gold wire surface. At first, visible growth is confined to the surface interface between the indium and the gold, and is of the fine-grained type noted on the surface of the compound layers formed at higher temperatures. After about 9 weeks at 40°C, blocky grains can be seen growing up through the indium. Indium depletion was complete in Figure 27 at 3 months; no further change occurred with additional holding time. The resulting blocky structure is loosely jumbled together with many voids, as perhaps the last indium to react migrates to some crystallographically preferred site at the expense of mechanical integrity. The area pictured in Figure 28 has virtually completed the reaction in 6 months time.

6 Growth Rate Curve Determination

The thickness of the intermetallic compound layer after various time-temperature exposures was determined by measurements taken from 1000× photographs of the polished cross-sections. At the higher temperatures (100°C and above) the layer thickness was non-uniform and considerable scatter in the data was observed. At temperatures of 80°C and lower, layer growth was more even; however, the percent error in measuring a thin layer is higher. The difficulty of preparing the metallographic specimens also contributes to the scatter in the measurements.

The resulting data were plotted in Figure 29 as layer thickness versus hours at temperature, and a linear time-temperature relationship was assumed.

Reaction layer thickness measurements were then plotted as micrometer per hour versus the reciprocal of the holding temperature and a straight line resulted when the graph was plotted on semi-log paper (Figure 30). From this graph the equation for the reaction rate, β, was found to be

$$\beta = (6.88 \times 10^8 \ \mu\text{m/hr}) \cdot \exp\left(-\frac{0.72\,\text{eV}}{k_B T}\right) , \tag{1}$$

where k_B is the Boltzmann constant and T is the absolute temperature in kelvins. The activation energy is expressed as 0.72 eV.

For comparison, a similar curve derived for the reaction of lead-indium solder with gold by F. G. Yost et al. (Reference 3) is also presented in Figure 30. In both cases the bulk of the reaction layer consisted of $AuIn_2$. The reaction rates in both cases are also quite similar, and may well be the same if the variations in materials and technique between the two experimental programs could be fully taken into consideration.

It would appear that the reaction (formation of $AuIn_2$) proceeds as fast or nearly as fast in the presence of lead as it does when the reactants are gold and indium alone. This means that the body of literature which has been generated concerning the reactions of lead-indium solders with gold should be almost directly applicable to the gold-indium system, at least where conditions are such that the reaction product is primarily $AuIn_2$. In the presence of lead, Yost found that the individual grains of $AuIn_2$ were surrounded by a film of lead which rendered the alloy ductile, while in the present investigation, without lead, the $AuIn_2$ was extremely friable and crumbled readily. Thus, the mechanical properties of the reaction layers of the two alloy systems cannot be directly compared. A joint containing $AuIn_2$ and lead might be mechanically acceptable, whereas in the absence of lead, it would fail catastrophically.

6.1 Application of Results to Detector Bond Problem

Two further calculations which pertain directly to the detector bond problem which prompted this investigation were made:

1. How much $AuIn_2$ could result from current manufacturing techniques and room temperature storage, and
2. At what temperature does the reaction rate reach an acceptably low level for long term storage?

To answer the first question, reaction rates were taken from Figure 30 for the pertinent temperatures, and the following calculation was made:

From graph (numbers in square brackets [] are computed from the equation):

```
Growth rate at 20 C = .00023 um/hr.  [0.000225]
            at 70 C = .016   um/hr.  [0.0148]
            at 95 C = .096   um/hr.  [0.0787]
Processing:
        12 hours at 95 C = (12)(0.096) = 1.15 um/hr   [0.945]
       168 hours at 70 C = (168)(0.016)= 2.69 um/hr   [2.493]
                                         --------------------
                                         4.84 um/hr   [3.438]
Storage:
           1 year = (365)(24)(0.00023) = 2.0 um/year  [1.97]
```

Thus, if a device were stored at 20°C for 4 years, assuming an adequate supply of indium, the total reaction layer would be a maximum of 4.8 μm [3.44 μm] from processing plus (4×2.0) from storage for a total of 12.8 $\mu = 500$ micro-inch [11.3 μ] ($AuIn_2$ on NOAA AVHRR detector, 4 years old, was measured at 10 μm.)

These figures assume an infinite supply of gold and indium available for reaction. In actuality, the amount of indium in direct contact with gold can vary from zero to something approaching "infinite" depending upon how the indium layer is displaced during the bonding operation.

To determine what temperature a device must be stored at to limit the reaction layer to a certain thickness in a given amount of time (over and above what may have formed during processing) the equation for the growth rate of $AuIn_2$ was expressed as

$$\ln(\beta) = -[(8.41 \times 10^3)/T] + 20.35 \tag{2}$$

and solved for T to yield

$$T = -(8.41 \times 10^3)/[\ln(\beta) - 20.35] \tag{3}$$

As an example, to limit the growth to less than one micrometers in four years, we require that

$$\text{reaction layer thickness} = \text{ reaction rate} \times \text{ time, } t \leq 1\mu\text{m}\,, \tag{4}$$

or

$$\beta \cdot t \leq 1 \tag{5}$$

where $t = 3.504 \times 10^4$ hr (i./,e., the number of hours in four years). Thus,

$$\beta \leq 2.85 \times 10^{-5}\mu\text{m/hr} \tag{6}$$

$$\Rightarrow \ln(\beta) \leq -10.466\,. \tag{7}$$

Using this value of β in equation (3)

$$T \leq -(8.41 \times 10^3)/(-10.466 - 20.35) = -(8.41 \times 10^3)/(30.82) = 272.9\text{K} \tag{8}$$

Thus, the device must be stored at 0°C or less to limit additional growth to one μm in 4 years. Of course, this one micrometer thickness has been arbitrarily chosen for the sake of illustration; an "acceptable" value for layer growth is as yet undefined. It seems likely, however, that the reaction will continue, albeit slowly, at room temperature and below. It should also be remembered that, as further work at low temperatures (below 40°C) is completed, the graph may be subject to change. At these temperatures, months are required between measurements. (One measurement has been made at 40°C; none at room temperature.)

7 Conclusions

The work outlined in the memo of May 15, 1979, to the TIROS Project Office, Mr. Draper, has been completed and is herein reported. The preliminary conclusions presented in the above memo have been supported, and a growth rate curve determined from which room temperature extrapolations may be obtained. Conclusions which apply to detector bonds are summarized as follows:

1. The growth rate of $AuIn_2$ is not negligible at room temperature.
2. Current processing techniques are very likely to form significant amounts of $AuIn_2$.
3. The reaction product $AuIn_2$ occupies more space than did the reactants and its presence can lead to fracture or separation of the bonded area.
4. The reaction product is a good electrical conductor, and, provided mechanical integrity in the bond area is maintained, its presence would not affect the operation of the device.
5. The mechanical properties of the reaction layer are very poor; it tends to form loosely bonded blocky crystals and is extremely friable.
6. From conclusions 4 and 5, there is no non-destructive way of determining whether a properly functioning device has very weak bonds.
7. Long term storage of detectors with gold and indium in the bond area should be at low temperature — the exact temperature being determined by what is considered an acceptable growth rate. (Going from 20°C to 0°C retards the growth rate by about a factor of 3 [8.22]).

8 Recommendations

1. Existing detectors should be stored at as low a temperature as is feasible. Ordinary refrigerator or preferably freezer temperatures may be adequate. Elevated temperature bakeouts should be minimized.
2. Recent work by Shih and Ficalora (Reference 4) showed that intermetallic growth in several binary systems such as Au-Al is severely retarded or eliminated by a hydrogen atmosphere. The effect of H_2 on Au-In reactions as well as on detector performance should be investigated.
3. The present work assumes that an infinite supply of gold and indium is present for reaction. Actual detector bonds will vary greatly in the extent of Au-In contact areas. A large number of realistic bonds should be prepared, exposed to various times at temperature, mechanically tested, and sectioned to give a better idea of what a typical detector bond is like.
4. In future detectors, the gold-indium system should be avoided if performance specifications permit.

9 Acknowledgments

Many thanks to Carl Haehner, Carr Walch, and Joanne Uber for designing and building the shear test fixture and for conducting the shear tests, and to Richard Marriott for the derivation of the growth rate equations.

10 References

1. G. W. Powell and J. D. Braun, *Diffusion in the Gold-Indium System*, Trans. AIME, Vol. 230, June 1964, 694–699.
2. F. A. Shunk, *Constitution of Binary Alloys*, Second Supplement, McGraw-Hill Book Co., 1969.
3. F. G. Yost, F. P. Ganyard, and M. M. Karnowsky, *Layer Growth in Au-Pb/In Solder Joints*, Metallurgical Transactions A, Volume 7A, August 1976, 1141–1148.
4. D. Y. Shih and P. J. Ficalora, *The Reduction of Au-Al Intermetallic Formation and Electromigration in Hydrogen Environments*, Proc. 1978 Annual Reliability Physics Symposium, p. 268.

signed:
Jane E. Jellison
(signature on file)

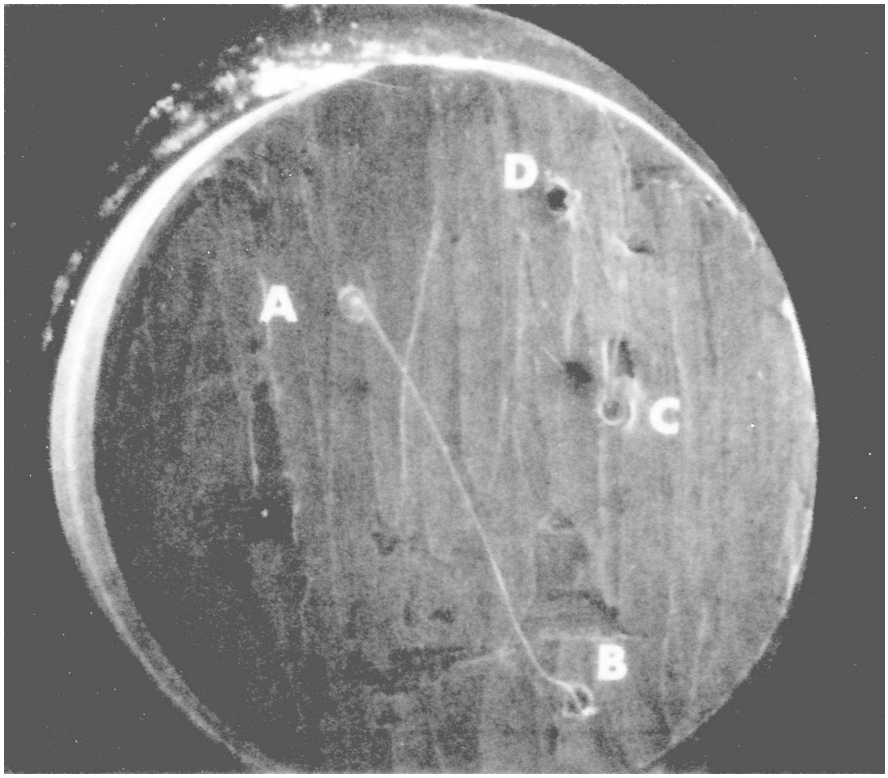

Figure 1: Bond specimen #1 (after pull testing) showing location of bond pairs. Bonds A and D are ball bonds, while bonds B and C are wedge bonds. The wedge bond B and the ball bond D have lifted in this image. 15×

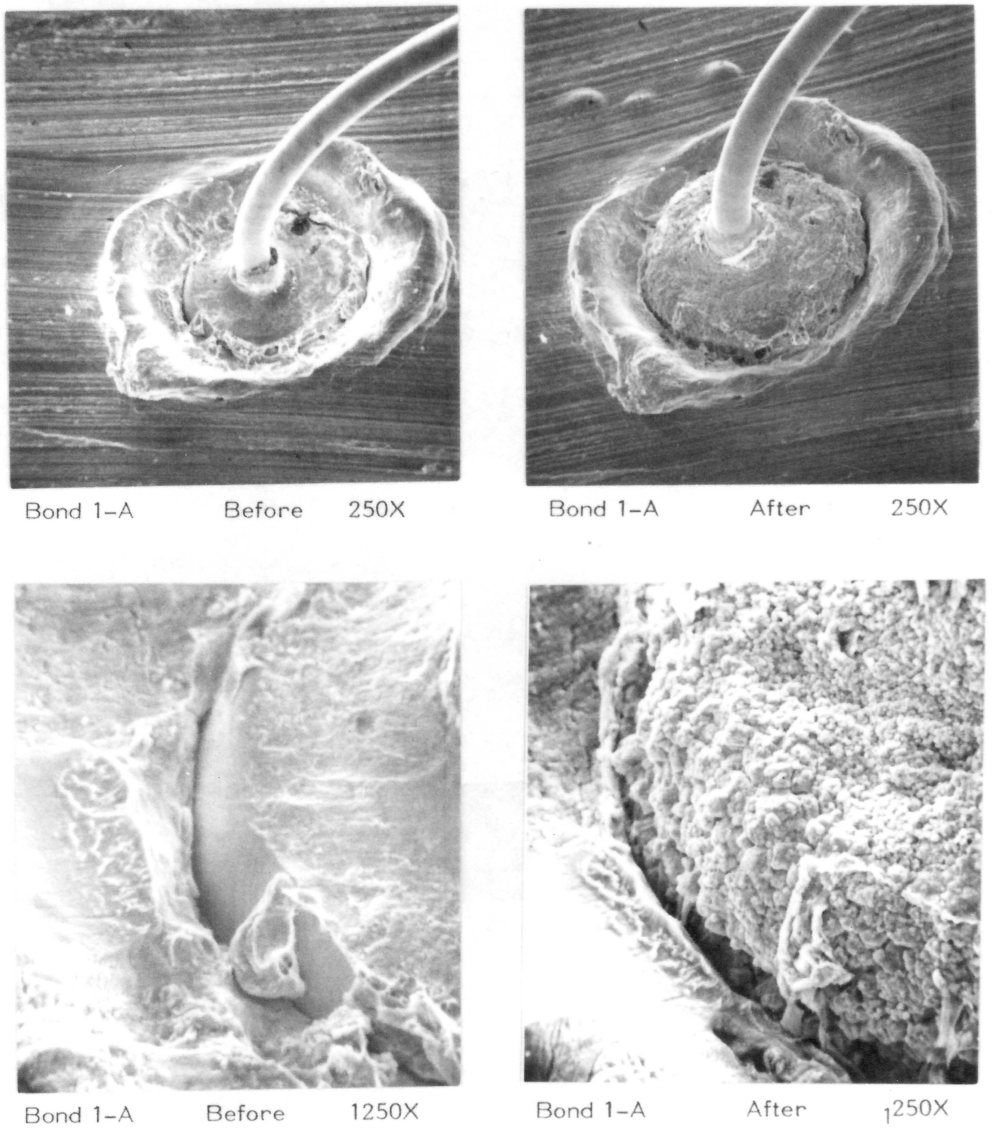

Figure 2: Bond 1-A before (left) and after (right) exposure to 73 hours at 140°C and 97 hours at 120°C. Surface of gold ball is covered with crystalline growth.

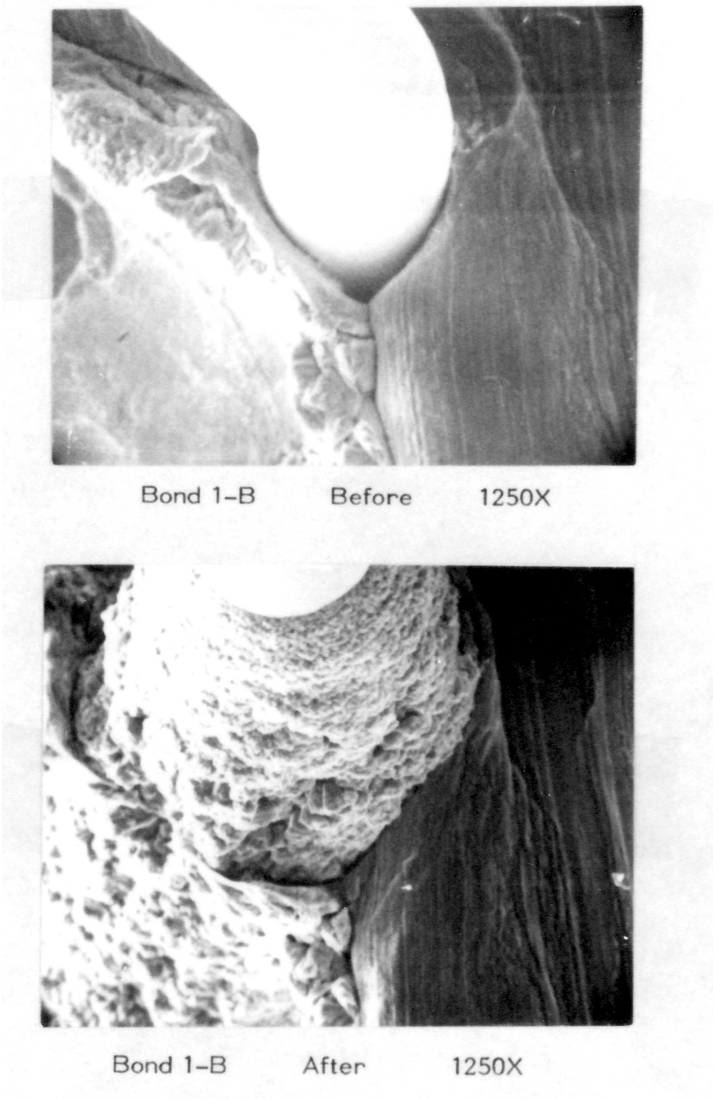

Figure 3: Bond 1-B before and after elevated temperature exposure. Compound growth has extended upward on the surface of the gold wire.

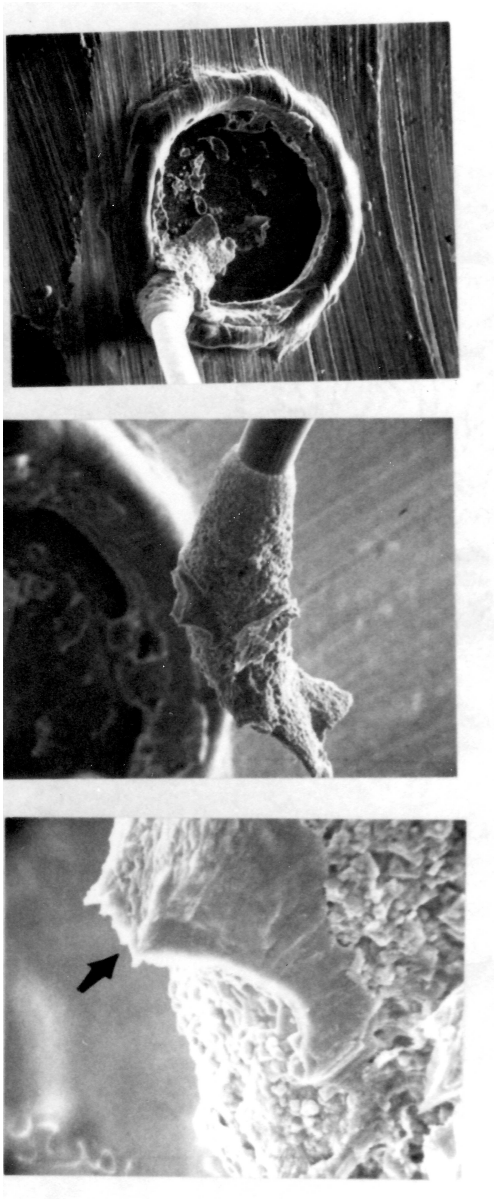

Figure 4: Top image, 250×: Bond 1-B after 73 hours at 140°C plus 97 hours at 120°C. Middle image, 500×: Bond 1-B after temperature exposure and pull testing. Most of the under surface of the wire is covered with intermetallic compound. Bottom image, 2,500×: The arrow points to an area of ductile failure in indium at the heal of the bond.

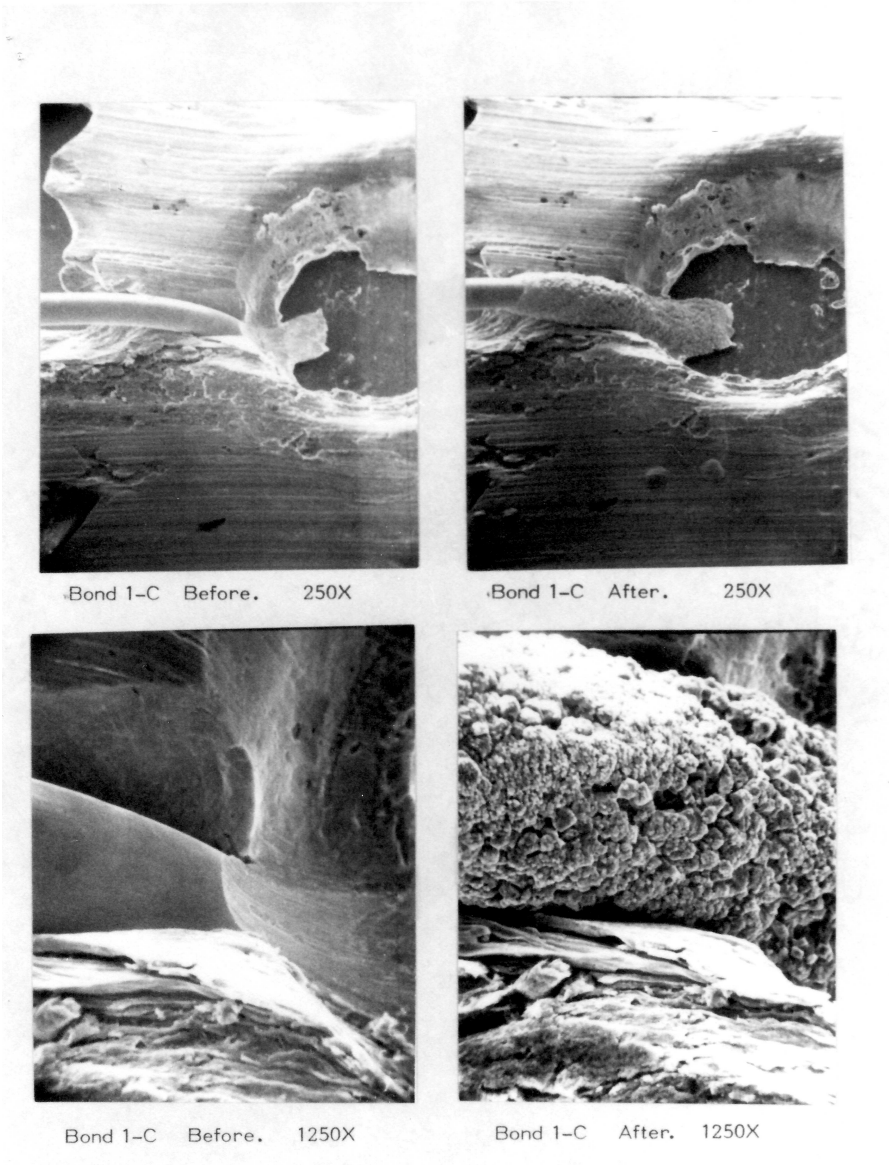

Figure 5: Bond 1C before and after exposure to 140°C. Thick coating of crystalline growth surrounds wire near bond area.

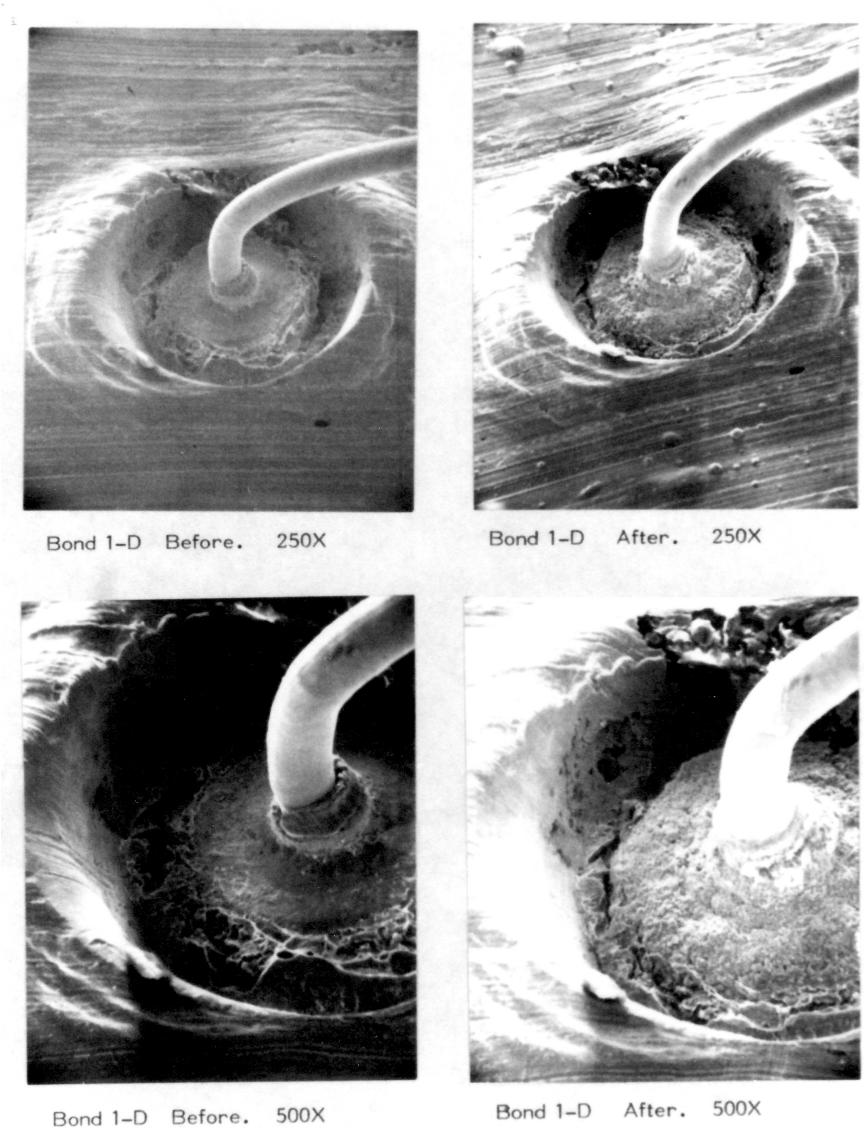

Figure 6: Bond 1D before and after exposure to 140°C. Extensive coverage of gold ball by crystalline growth.

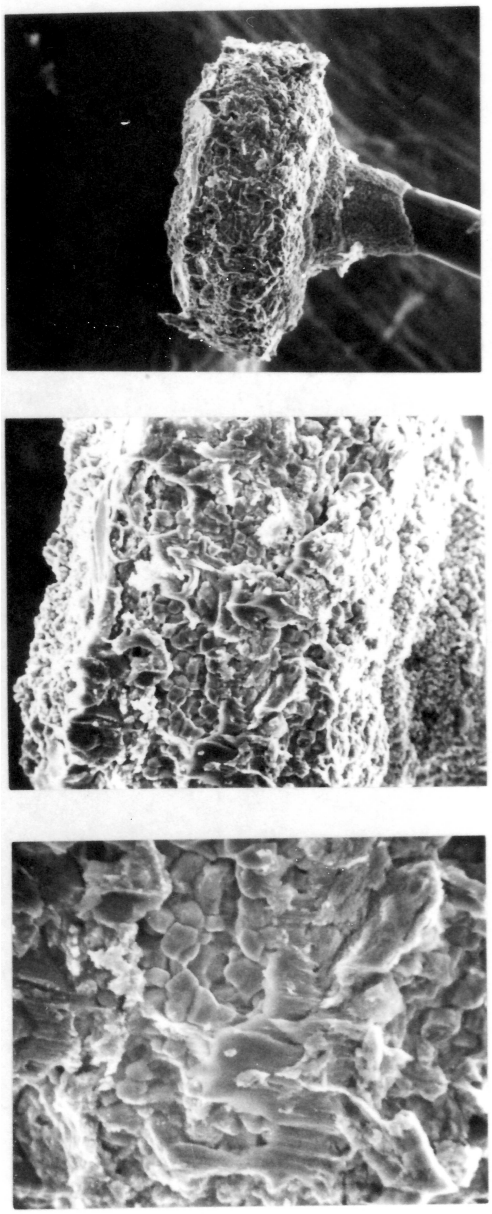

Figure 7: Top image, 500×: Bond 1D after pull testing. Bond lifter at 2 g_f load. Middle image, 1,250×: Blocky grains of intermetallic compound on all ball surfaces. Bottom image, 2,500×: Higher magnification view of blocky grains mixed with ductile failure of indium.

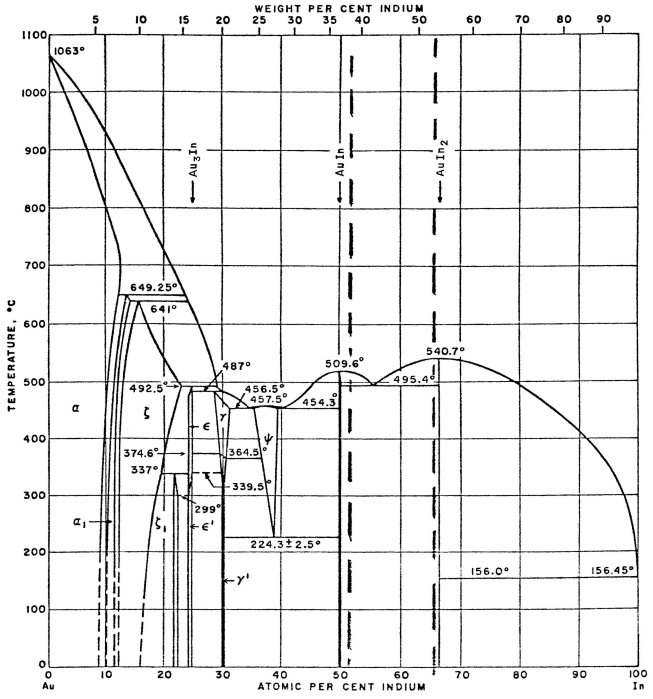

Figure 8: Phase diagram for the gold-indium system (Ref. 2). The compounds prepared in this study (whose composition is shown by the dotted lines) were chosen slightly inside the boundaries of the AuIn-$AuIn_2$ eutectic region to avoid the presence of other phases.

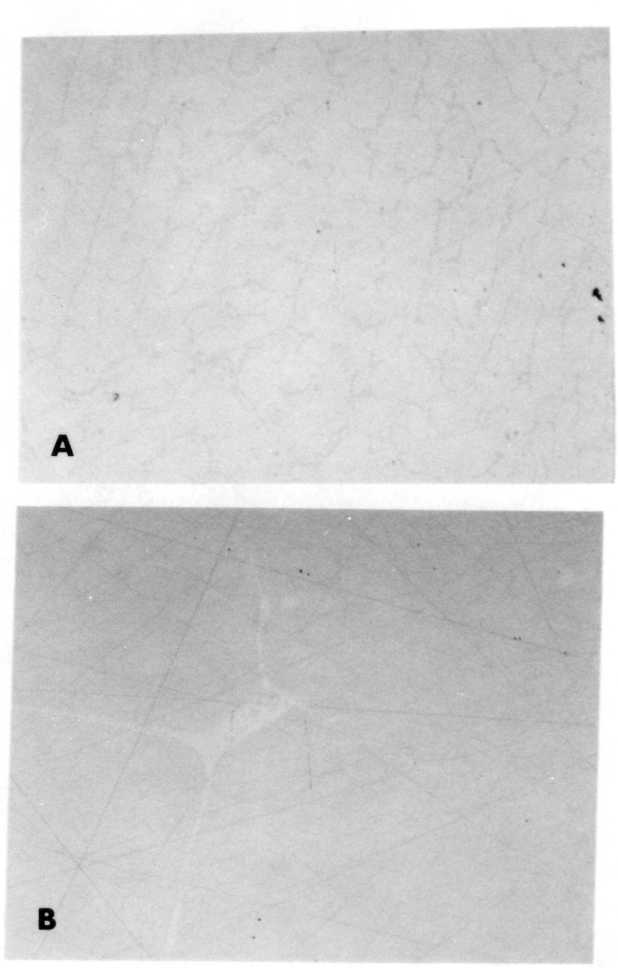

Figure 9: Microstructures of compounds at 100 $\times$, unetched. Top image, A: AuIn matrix with $AuIn_2$ network. Bottom image, B: $AuIn_2$ matrix with AuIn at grain boundaries.

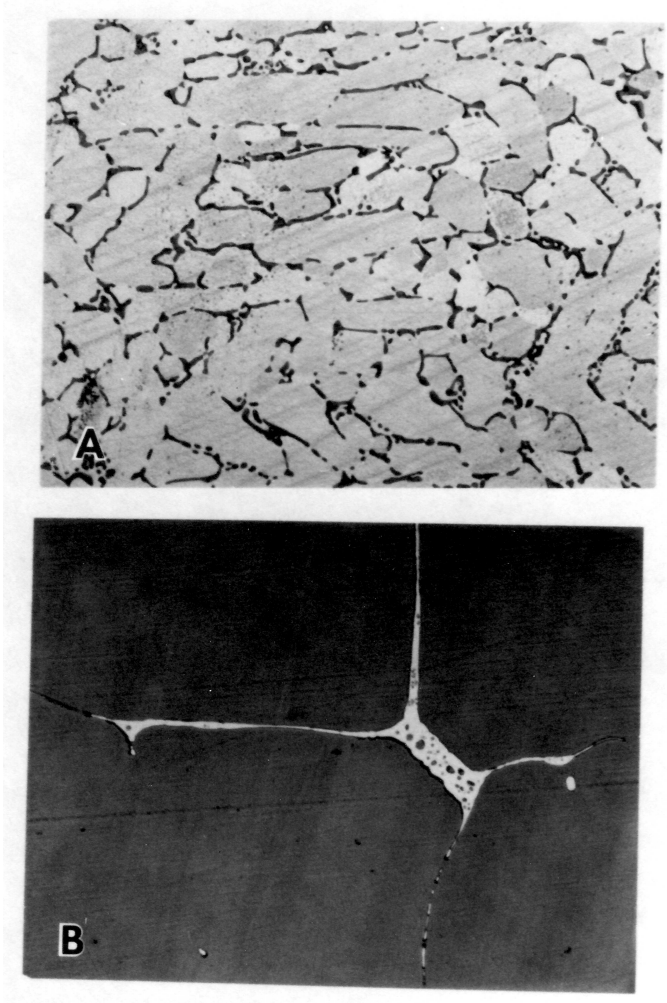

Figure 10: Microstructures of compounds at 100 $\times$, etched. $AuIn_2$ etches dark; AuIn remains light. Etchant: 100 mL acetic acid, 2/3 mL hydrofluoric acid, 33 mL nitric acid, 2 mL hydrochloric acid. Top image, A: AuIn matrix with $AuIn_2$ network. Bottom image, B: $AuIn_2$ matrix with AuIn at grain boundaries (this is the same field as Figure 9B, but rotated 90 degrees clockwise).

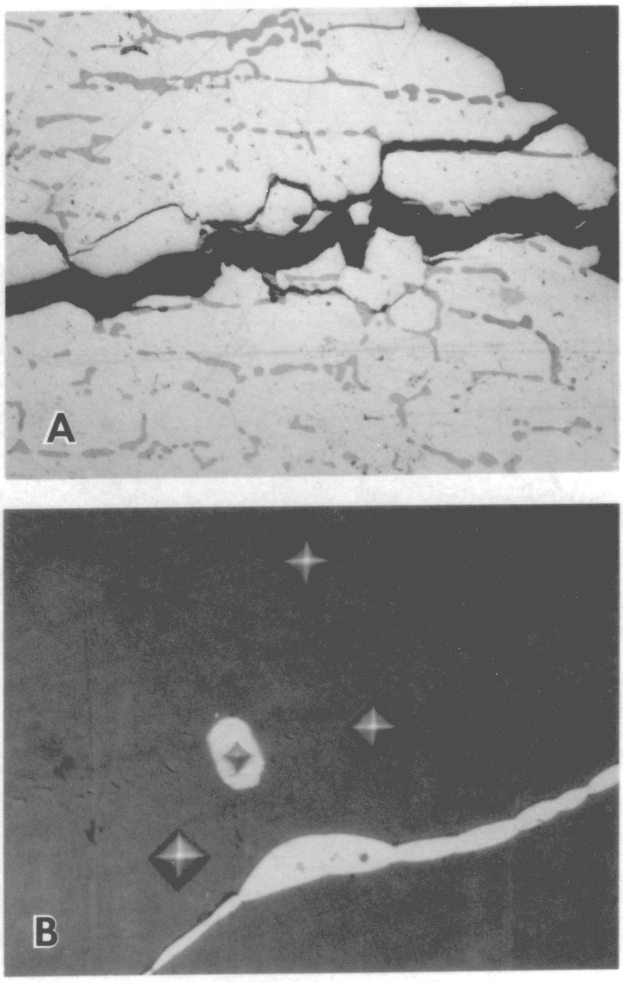

Figure 11: Microstructure of intermetallic compounds, etched. Top image, A: Brittle cracks in both AuIn and $AuIn_2$ phases. Bottom image, B: Microhardness indentations in AuIn (light) and $AuIn_2$ (dark) phases. A larger indendation indicates a softer material.

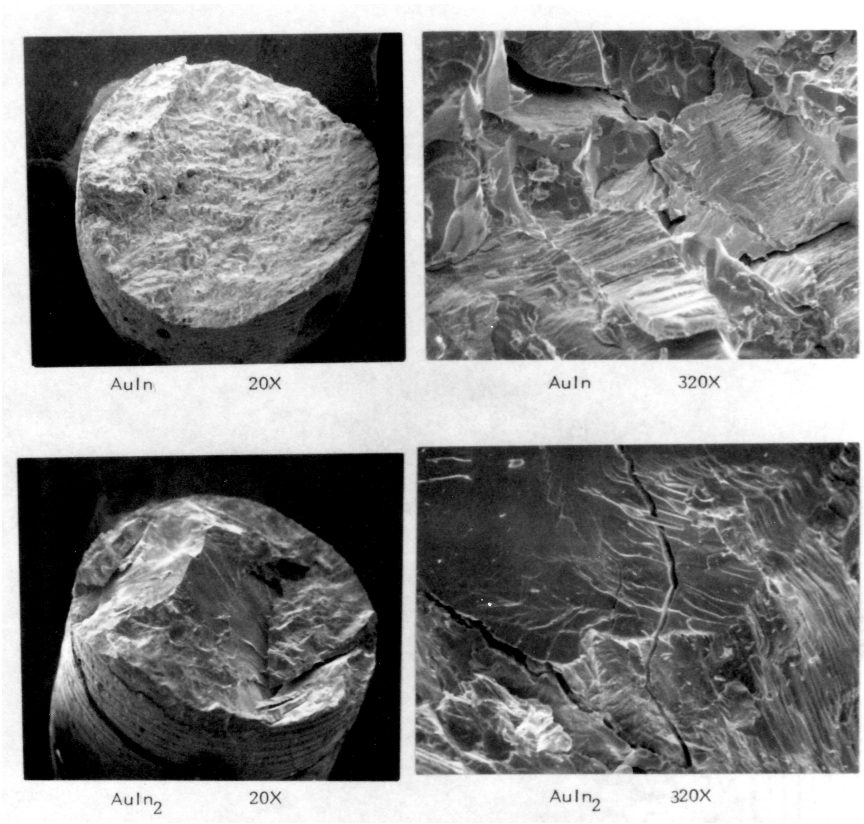

Figure 12: SEM Fractographs of AuIn and $AuIn_2$ ingots after shear testing. Both phases fractured in a brittle manner by cleavage.

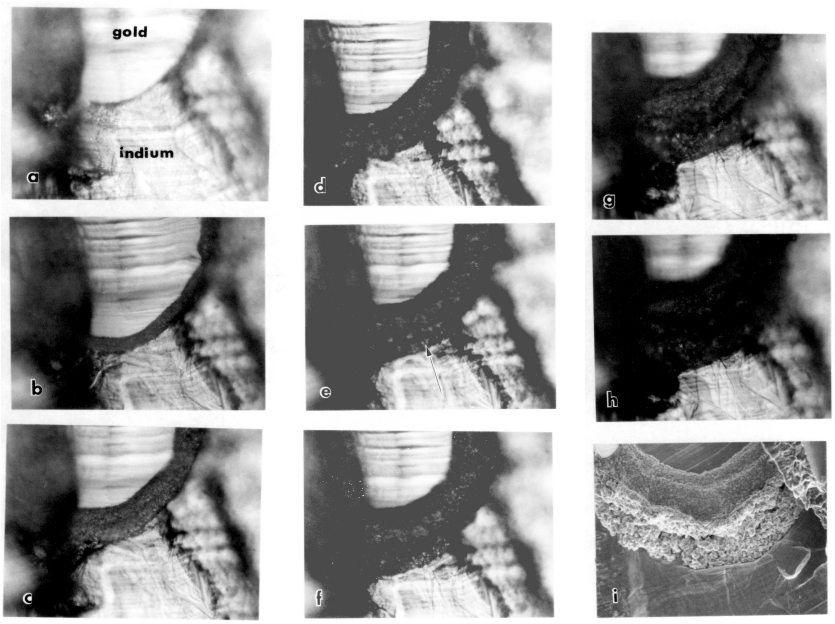

Figure 13: Hot stage optical microscope specimen, at 400×. Left top image, a: 15 minutes. Reaction product starting to grow at interface. Left middle image, b: 1.5 hours. Dark layer has spread. Left bottom image, c: 3 hours. Dark layer is consuming and/or covering both gold and indium surfaces. Center top image, d: 7 hours. Center middle image, e: 14 hours. Blocky grains visible in fissure (Arrow). Center bottom image, f: 21 hours. Right top image, g: 28 hours. Right middle image, h: 35 hours. Right bottom image, i: 35 hours, SEM photograph at 640×.

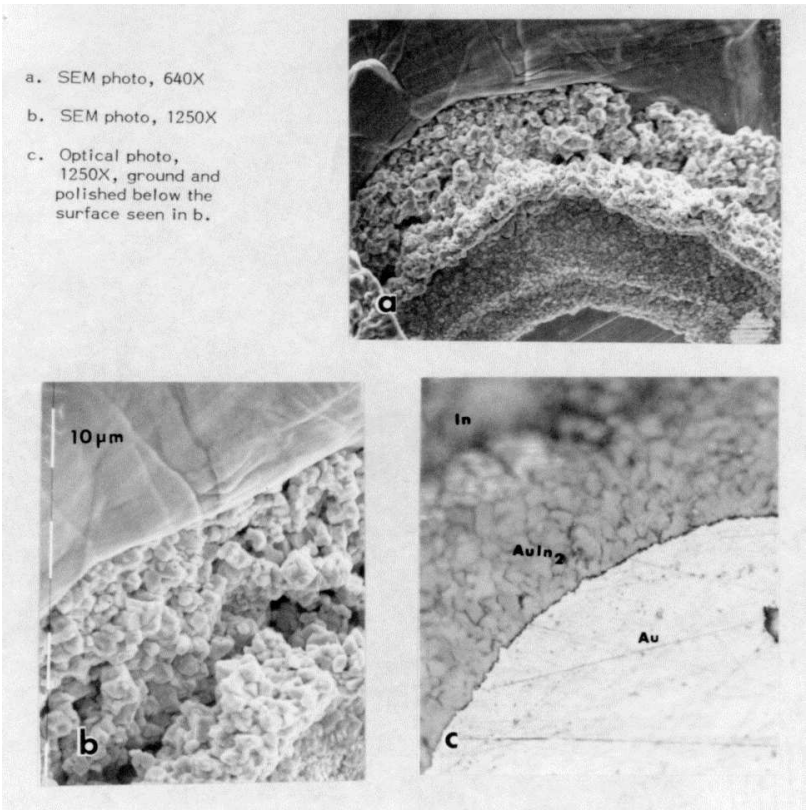

Figure 14: SEM photographs of surface compared with optical photographs of cross section through hot stage specimen.

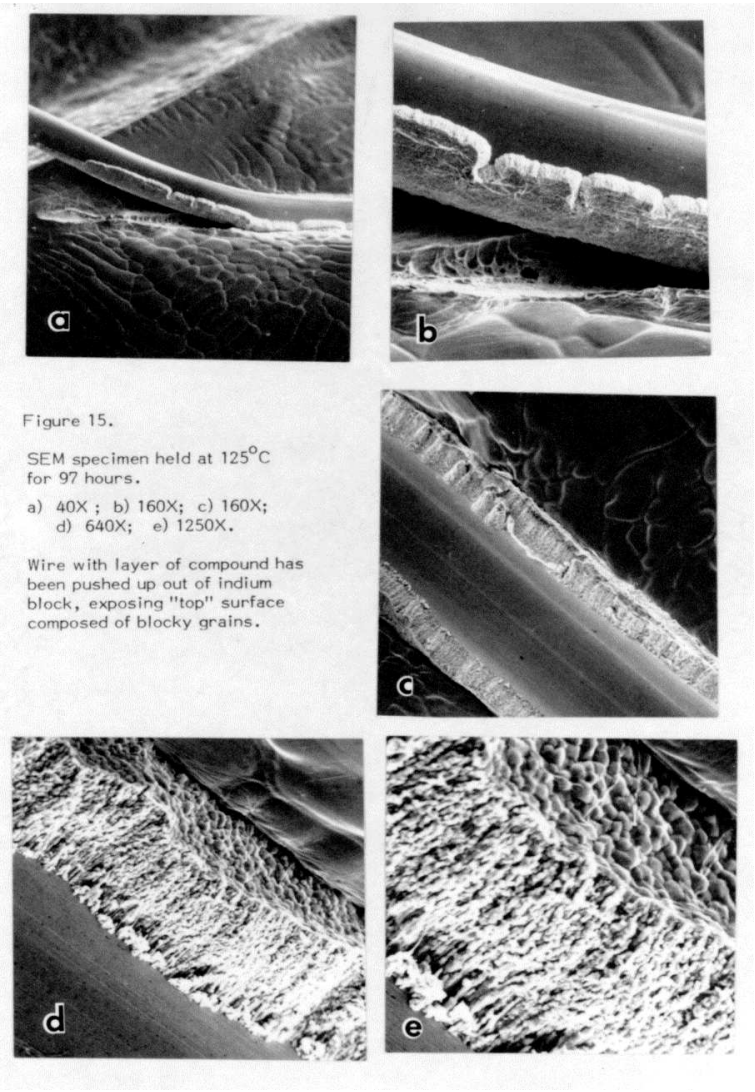
a
b
c
d
e
Figure 15.
SEM specimen held at 125°C for 97 hours.
a) 40X ; b) 160X; c) 160X; d) 640X; e) 1250X.
Wire with layer of compound has been pushed up out of indium block, exposing "top" surface composed of blocky grains.

Figure 15:

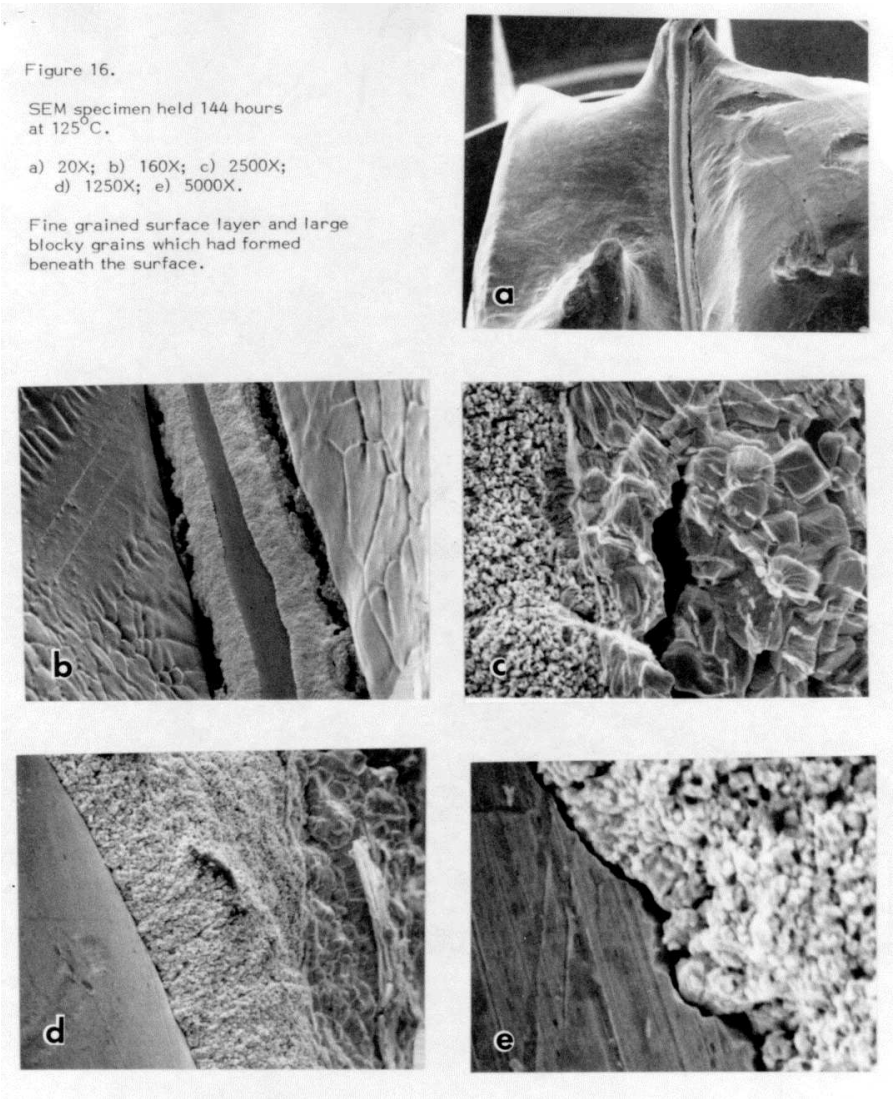
Figure 16.
SEM specimen held 144 hours at 125°C.
a) 20X; b) 160X; c) 2500X; d) 1250X; e) 5000X.
Fine grained surface layer and large blocky grains which had formed beneath the surface.
a
b
c
d
e

Figure 16:

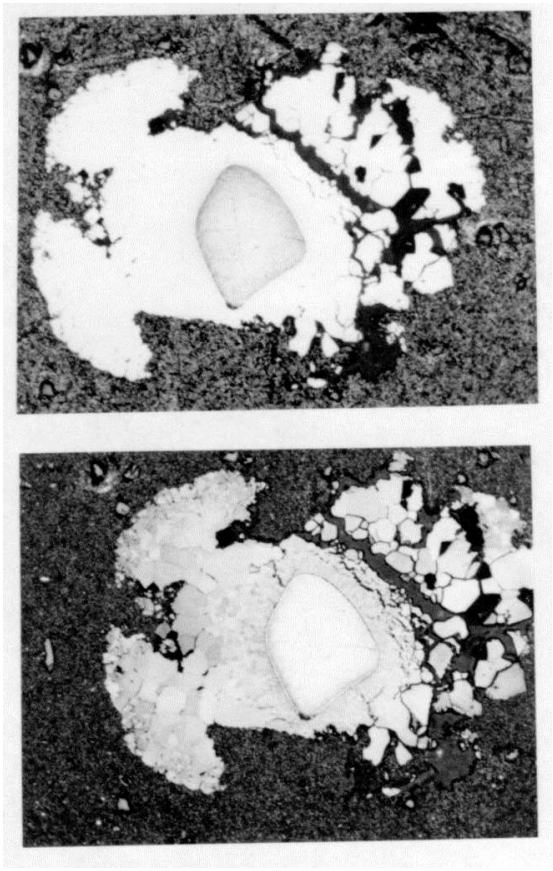

Figure 17: Cross section through specimen held at 125°C for 500 hours in the unetched (top image) and etched (bottom image) condition. Compound growth is very irregular and consists almost entirely of $AuIn_2$.

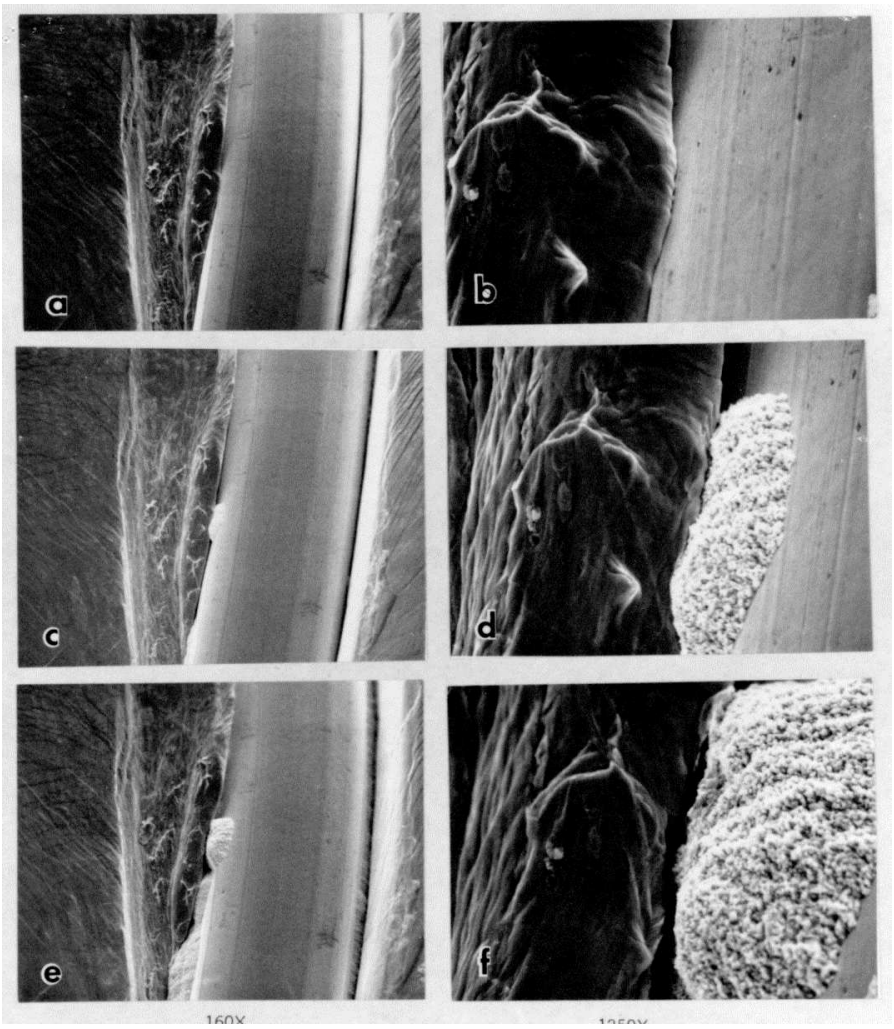

Figure 18: SEM specimen held at 100°C for the indicated times: images a & b for 0 hours; images c & d for 72 hours; and images e & f for 240 hours. A patch of Au-In compound developed where gold and indium were in close contact.

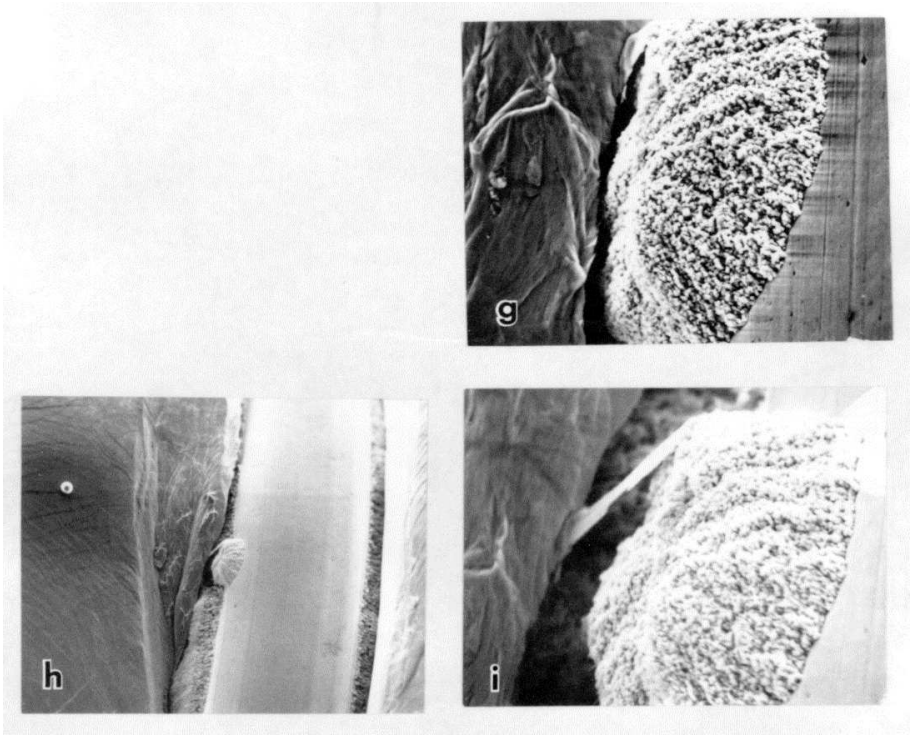

Figure 18: (continued) SEM specimen held at 100°C for the indicated times: image g for 312 hours, and images h & i for 568 hours. Continued growth beneath the wire has forced the compound patch area away from the indium and further patch grwoth ceased.

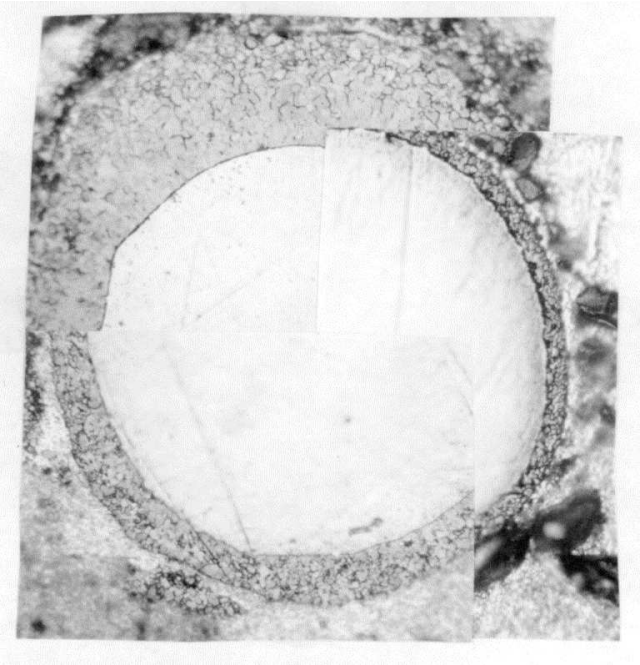

Figure 19: Composite photograph at 500× showing growth of intermetallic compound at 100°C. Clockwise: 72 hours→ 1 to 5 o'clock; 144 hours→ 5 to 9 o'clock; and 240 hours→ 9 to 1 o'clock.

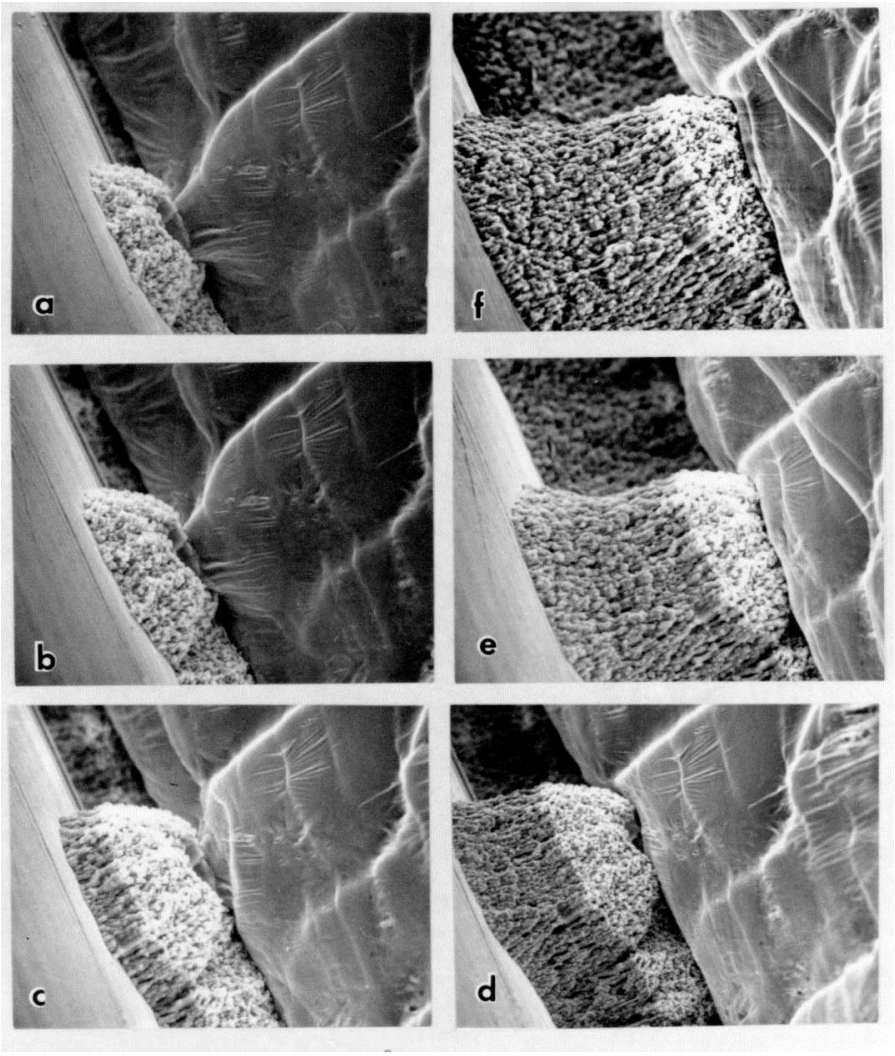

Figure 20: SEM specimen held at 80°C for the indicated times: image a for 164 hours; image b for 209 hours; image c for 357 hours; image d for 672 hours; image e for 900 hours; and image f for 1,072 hours. All images are at 1,250×. Demonstrates plastic deformation of the bulk indium caused by compound growth.

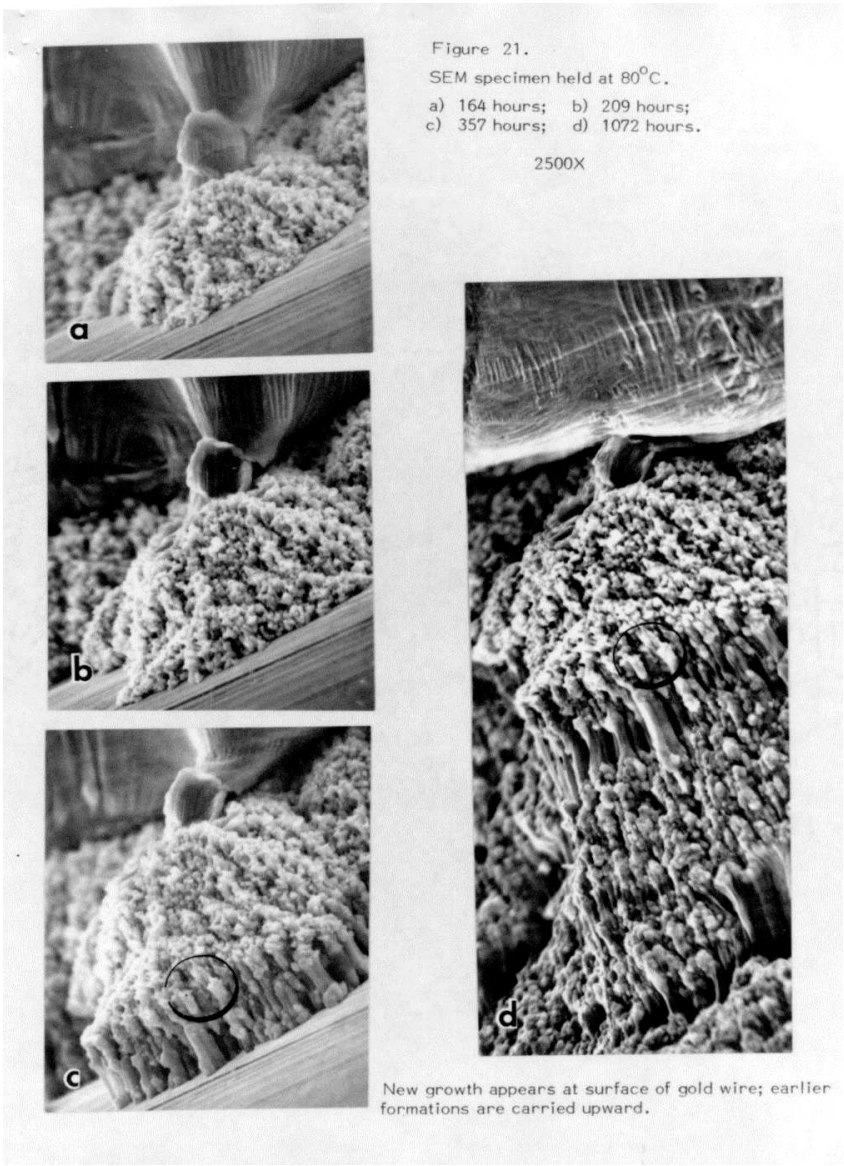
Figure 21.
SEM specimen held at 80°C.
a) 164 hours; b) 209 hours;
c) 357 hours; d) 1072 hours.
2500X
a
b
c
d
New growth appears at surface of gold wire; earlier formations are carried upward.

Figure 21:

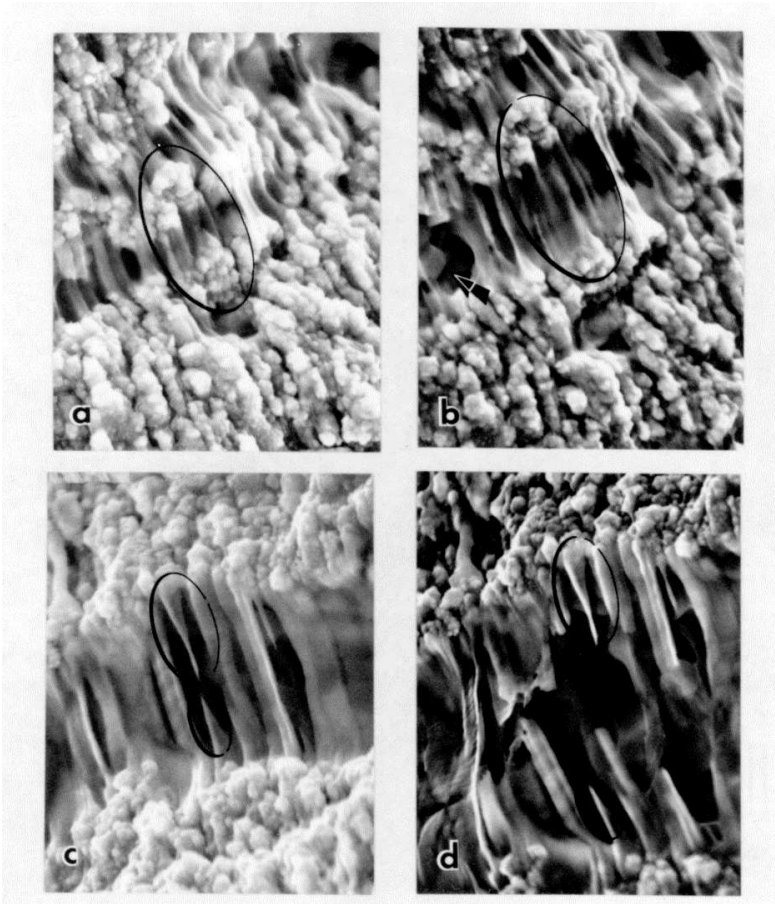

Figure 22. SEM specimen held at 80°C. Circled areas show ductile elongation of surface features. All at 5000X.

Figure 22:

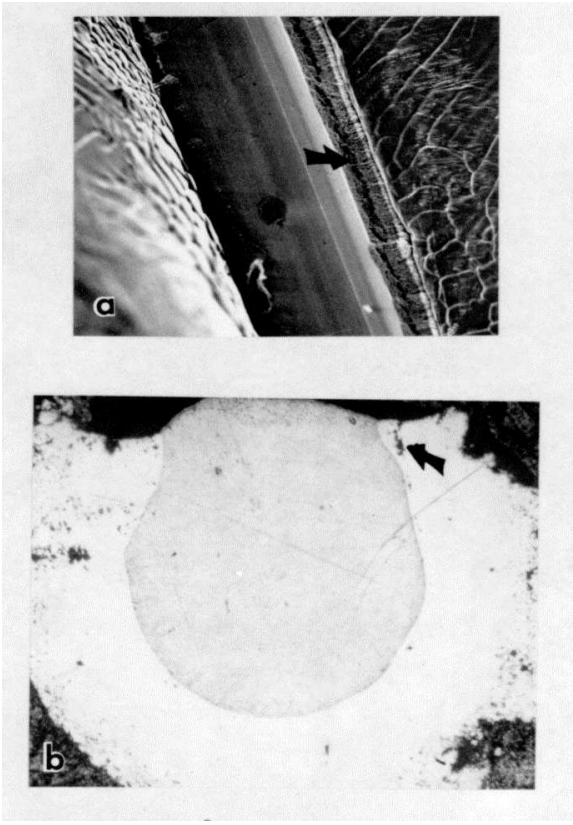

Figure 23: SEM specimen held at 80°C for 1,072 hours. Image a: SEM photograph at 160×; the arrow points to a fissure. Image b: Cross section through this area at 400×. Crack at arrow corresponds to fissure in image a.

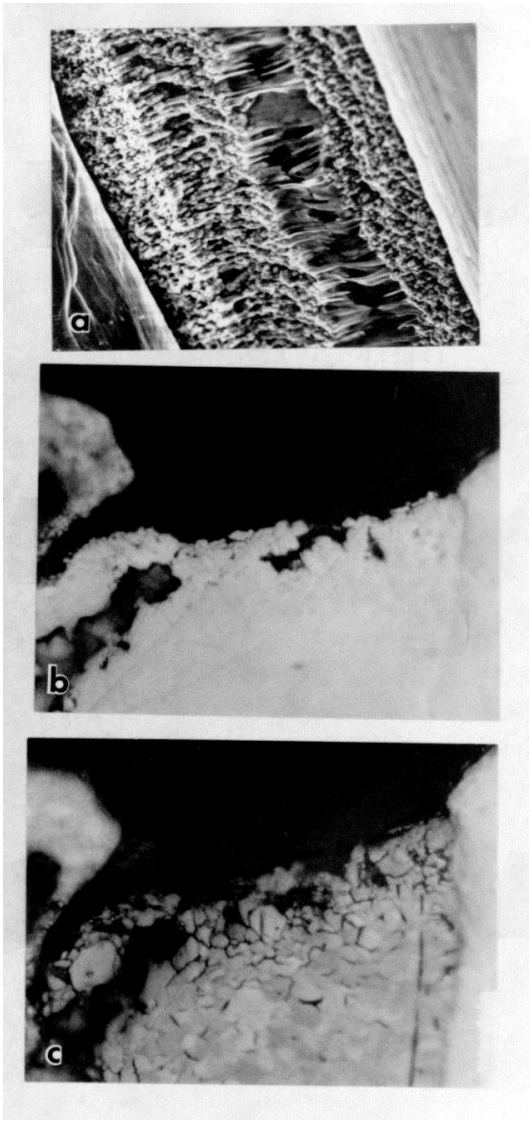

Figure 24: Top image, a: SEM specimen held at 80°C for 1,072 hours. Middle image, b: Cross section through an area as in image a, unetched, 1,250×. Bottom image, c: Area b etched, showing blocky grains of $AuIn_2$.

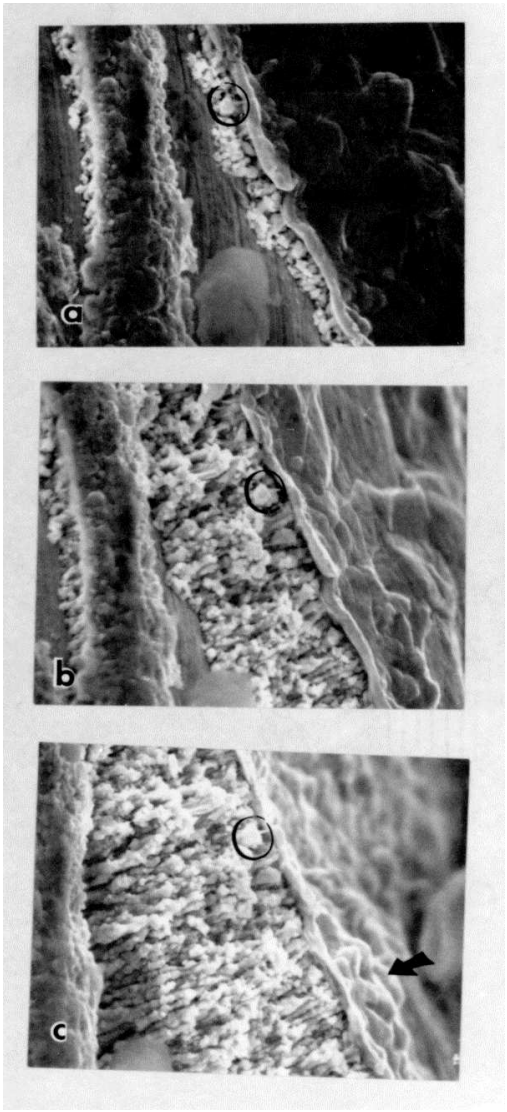

Figure 25: SEM specimen held at 80°C. Compound growth at an area where a thin layer of indium covered the gold. Arrow indicates blocky granis visible through thin film remaining unreacted. All images at 2,500×. Top image, a: 68 hours. Middle image, b: 154 hours. Bottom image, c: 357 hours.

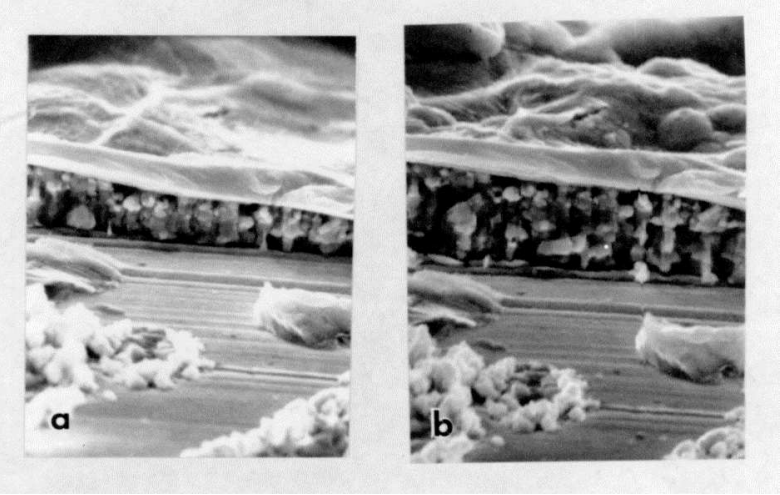

Figure 26: SEM specimen hald at 40°C for 4 months (image a) and for 6 months (image b). Layer growth is proceeding as at higher temperatures.

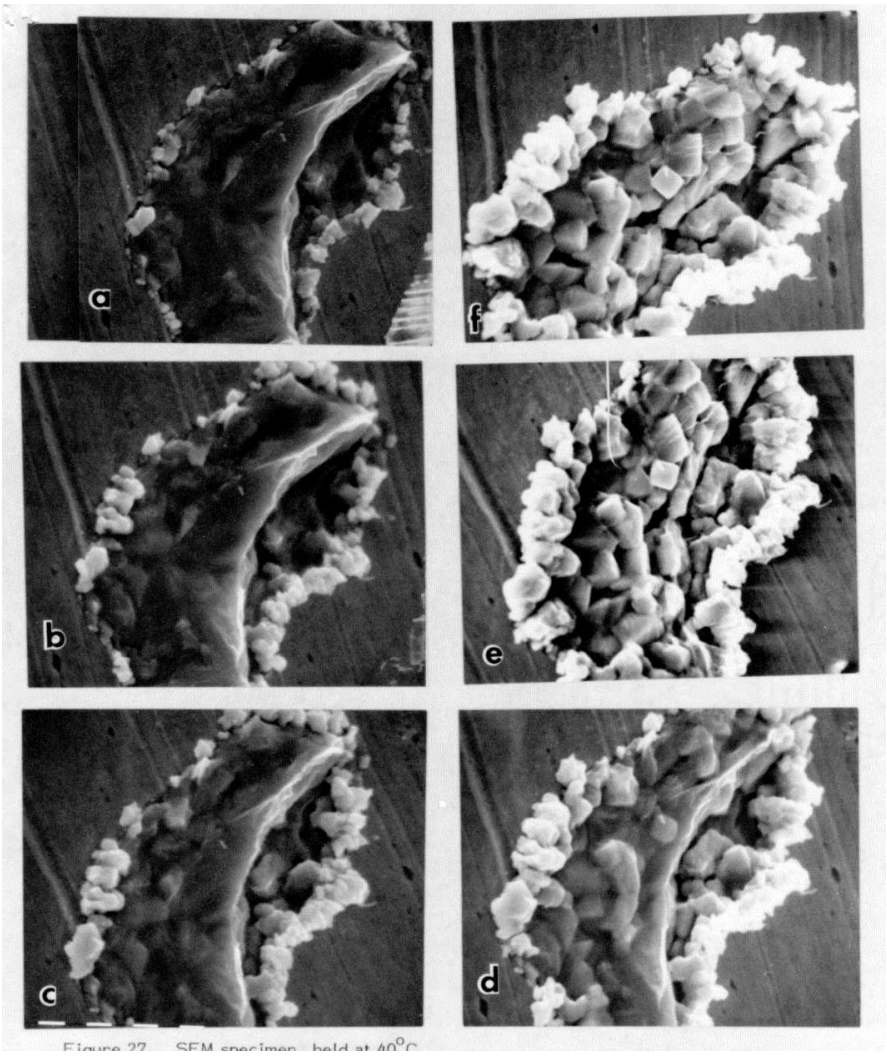

Figure 27: SEM specimen held at 40°C for 2 weeks (image a); 4 weeks (image b); 6 weeks (image c); 9 weeks (image d); 3 months (image e); and 4 months (image f). All at 5,000×. Final product is loosely connected grains of $AuIn_2$ which would be very poor mechanically.

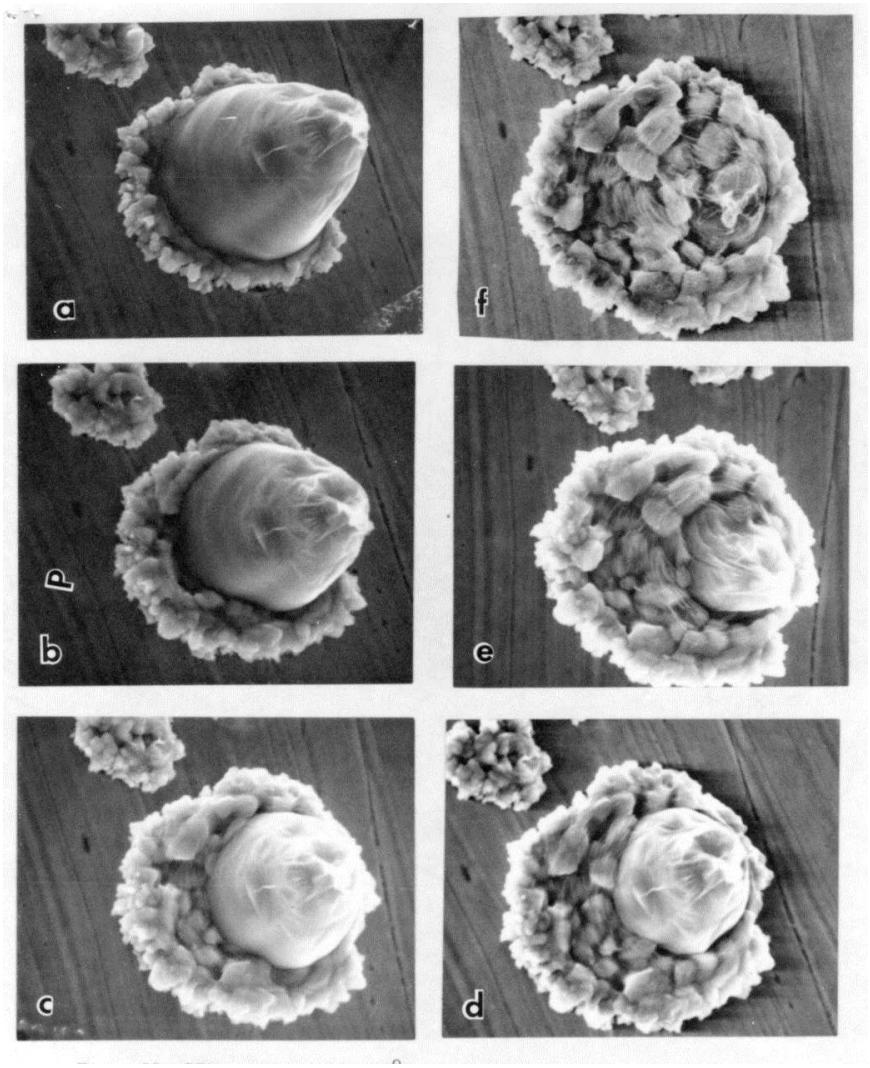

Figure 28: SEM specimen held at 40°C for 3 weeks (image a); 6 weeks (image b); 9 weeks (image c); 3 months (image d); 4 months (image e); and 6 months (image f). All at 5,000×. Formation of blocky $AuIn_2$ almost complete after 6 months.

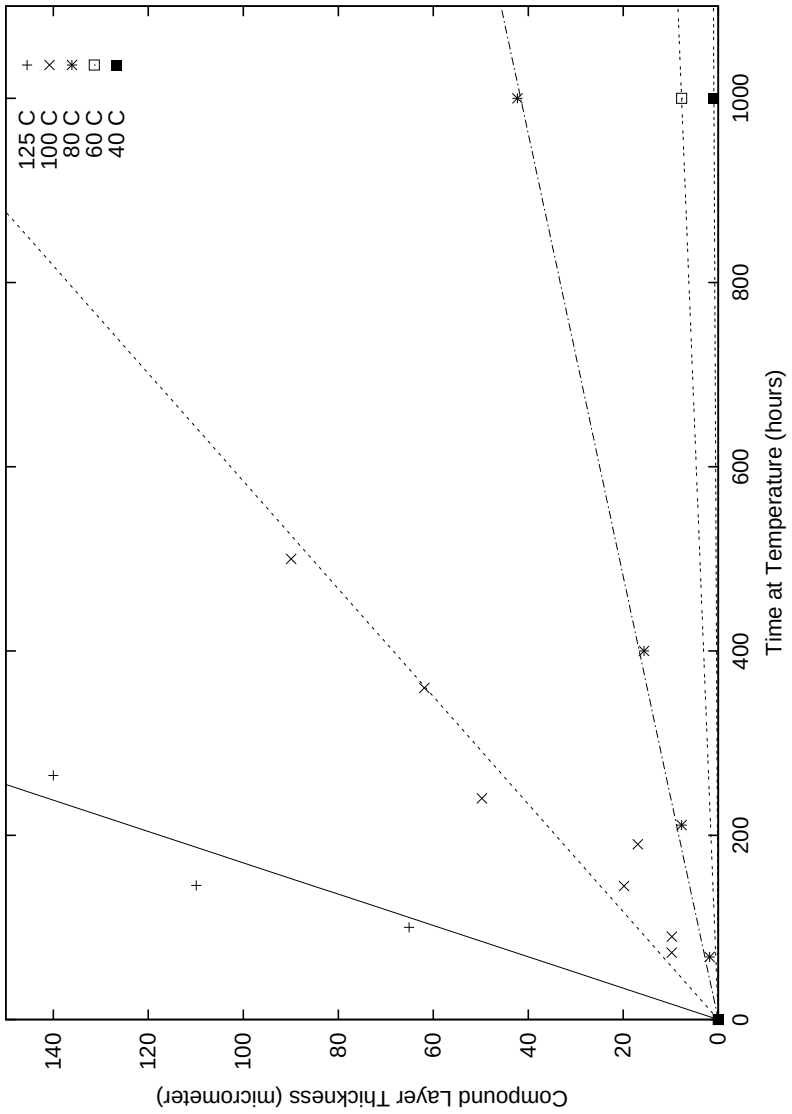

Figure 29: Plot of the thickness h of the intermetallic Au-In compound at selected times t up to 1,000 hours, for specimens held at selected temperatures, T. The least-square fitted lines are also shown: $h = \beta(T) \cdot t$; $\beta(125°\mathrm{C}) = 0.588$ μm/hr $\pm$ 9%; $\beta(100°\mathrm{C}) = 0.171$ μm/hr $\pm$ 6%; $\beta(80°\mathrm{C}) = 0.0416$ μm/hr $\pm$ 2%; $\beta(60°\mathrm{C}) = 0.00773$ μm/hr; and $\beta(40°\mathrm{C}) = 0.00092$ μm/hr. The uncertainty of the last two values for β are roughly 10%, based on the difficulties of measuring the thickness of the single specimen at 40°C and at 60°C.

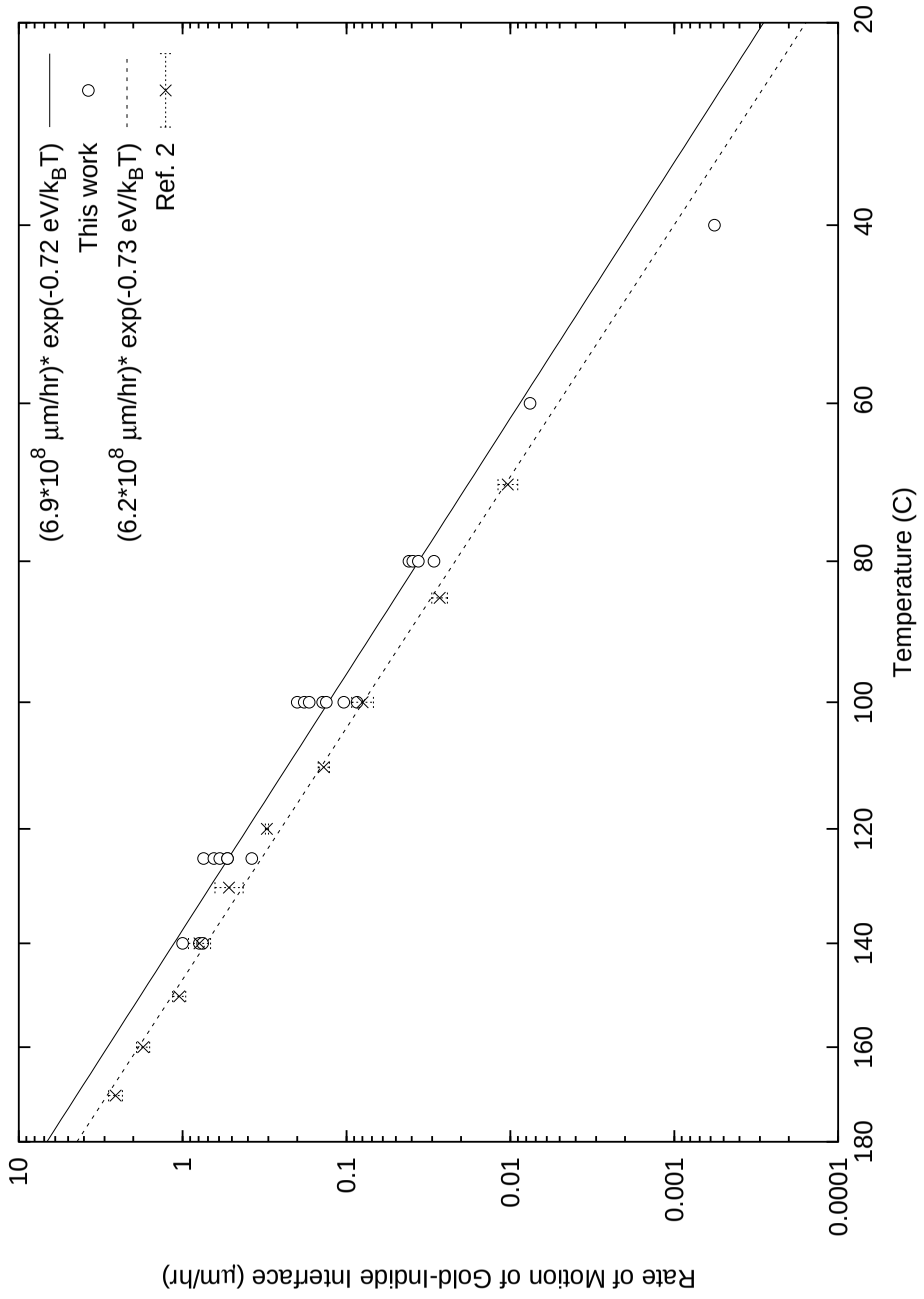

Figure 30: Arrhenius plot of rate of motion of gold-indium interface. "This work" labels data acquired in this study, a few of which were shown in the previous figure.